Sustainable deep soil mixing using GGBS–dolomite based geopolymer for soft ground improvement

Sanjoli Gupta [1*], and *Suresh* Kumar [1]

[1] Department of Civil Engineering, Indian Institute of Technology, BHU, Varanasi, India.

Abstract. The deep soil mixing (DSM) technique has been extensively adopted worldwide for soft ground improvement due to its effectiveness in reducing settlement, enhancing the stability of embankments over soft soils, and improving earthquake resilience. However, the conventional use of ordinary Portland cement (OPC) as a binder contributes substantially to carbon emissions. To address this environmental concern, this study investigates the potential of a sustainable industrial waste-based geopolymer binder composed of ground granulated blast furnace slag (GGBS) and dolomite, activated with sodium hydroxide (NaOH) and liquid sodium silicate (Na_2SiO_3), as a replacement for OPC in DSM columns, by conducting unconfined compressive strength analyses. Moreover, a series of laboratory model tests was conducted on embankments supported by groups of end-bearing geopolymer-stabilized soil columns (GPSCs) installed in very soft clay to simulate traffic loading. The test results were further validated through finite element analyses using PLAXIS 3D. The optimum mix, corresponding to a NaOH concentration of 8 M, NaOH: Na_2SiO_3 ratio of 25:75, liquid-to-precursor ratio of 1, and GGBS-to-dolomite (S:D) ratio of 16:4 (precursor/kaolin clay = 20%), achieved an unconfined compressive strength (UCS) of 1.47 MPa. The geopolymer-treated soft soil with an S:D ratio of 16:4 exhibited 26.30%, 32.59%, and 38.35% higher strength than the OPC20 specimens at 7, 14, and 28 days of curing, respectively. It was also found that the incorporation of end-bearing GPSCs in soft soil beds improved the stiffness and ultimate bearing capacity of the composite soft ground by 246.92% to 418.8% for area replacement ratios of 12.7%, 17%, and 21.2%. The finite element outcomes showed trends similar to the laboratory observations, validating the effectiveness of geopolymer-based DSM columns as a sustainable and high-performance solution for soft soil improvement.

1 Introduction

The construction of an embankment over soft soil requires implementing suitable ground improvement techniques to enhance the bearing capacity and stability of the ground beneath the embankment. Among numerous ground improvement techniques, deep soil mixing (DSM) has proven to improve the bearing capacity and reduce the settlement of soft or very soft soils. [1, 2]. The deep soil mixing (DSM) method of soft ground reinforcement has been used worldwide for several reasons, such as reducing settlements and increasing stability of the highway and railway embankments built over soft soils, enhancing the earthquake resilience of civil infrastructures, short realization time, and significant cost savings over alternative methods.

The DSM technique has been increasingly utilized to stabilize soft to very soft clays because it is rapid and economical to construct numerous infrastructure projects worldwide. Traditionally, OPC is used as a binder in the DSM process. In the process of cement manufacturing, substantial natural resources and energy are consumed, which contribute approximately 8–10% of global anthropogenic CO_2 emissions. Geopolymers offer comparable strength and durability for engineering applications and present a sustainable alternative to OPC [3–7]. The sodium/potassium-based alkali activator facilitates the geopolymerization process by dissolving the alumina and silica in the waste materials and forms calcium silicate hydrate (C-S-H), calcium aluminate hydrate (C-A-H), calcium aluminosilicate hydrate (C-A-S-H), or sodium aluminosilicate hydrate (N-A-S-H) gel [8]. Partial replacement of GGBS with dolomite has shown stronger durability performance, along with better resistance against sulfate attack, leaching, and carbonation, compared to using only GGBS as a precursor in the geopolymerization technique [9]. The addition of dolomite in alkali-activated GGBS results in the formation of a hydrotalcite phase that intermixes with the calcium aluminosilicate hydrate (C-A-S-H) gel at a very fine scale, improving the durability and strength of the matrix [10, 11].

Several researchers have conducted laboratory model studies to evaluate the behavior of groups of cement-stabilized deep mixing columns supporting rigid footings, embankments, and bridge abutments [12–16]. Full-scale field testing is costly and time-consuming, and laboratory testing is not always able to replicate

* Corresponding author: sanjoligupta.rs.civ19@itbhu.ac.in

complex field conditions. Consequently, numerical modeling has become an important tool for analyzing complex geotechnical problems. One of the most reliable and versatile numerical techniques for modeling embankment behavior is the finite element method (FEM). FEM-based evaluations provide for a comprehensive evaluation of bearing capacity, settlement characteristics, and overall stability under a range of loading conditions [17–20]. Horpibulsuk et al. [21]used finite element analysis in PLAXIS 2D along with 1-g laboratory model testing to examine the consolidation behavior of composite soft clay foundations. In order to assess the impact of variables including column length and stiffness, area replacement ratio, and permeability on stress concentration, settlement, and consolidation behavior of column-supported ground, Jiang et al. [22] carried out parametric numerical simulations using ABAQUS. In order to examine the settlement behavior of floating DSM columns, Liu et al. [23] conducted a series of laboratory model tests and finite element studies. The findings indicate that the degree of consolidation of ground stabilized by floating DSM columns is 10–20% less than that of end-bearing DSM columns.

Even though a lot of study has been done to understand the consolidation properties of soft soils treated with DSM, the majority of studies that have been done so far have mostly concentrated on the long-term performance of the deep mix column stabilized composite ground [13, 22, 24]. However, limited research has been conducted on the short-term performance of DSM-treated soils subjected to rapid loading conditions, such as those occurring during construction activities, traffic loading, or sudden surcharge application. Furthermore, while several analytical and numerical investigations have examined parameters such as column spacing, diameter, binder composition, strength development, and area replacement ratio, relatively few studies have validated these findings through experimental or field-scale observations. Such validation is essential to ensure that numerical simulations accurately represent actual field behavior.

In the present study, an attempt has been made to study the efficacy of GGBS and dolomite-based geopolymer with NH and NS as an alkali activator as a binder in place of OPC in the deep soil mixing technique. A series of four instrumented embankment model tests was conducted, one test on an untreated soft soil embankment model and three tests on groups of end-bearing GPSCs with different area replacement ratios (A_r) in very soft clay with an undrained shearing strength of 5±1 kPa, subjected to static loading conditions. The failure pattern of the GPSCs was observed by investigating the deformed shape of the GPSCs after the completion of the model tests. Furthermore, three-dimensional finite element analyses of embankment models on soft ground improved with GPSCs under static loading have been conducted to validate the measured embankment model test results.

2 Materials and methodology

2.1 Foundation and embankment soil

Commercially available kaolin clay, characterized by low swelling and shrinkage potential, was used to prepare the soft clay foundation bed. Silty sand was adopted as the embankment fill material in accordance with the recommendations of the RDSO (2020) guidelines. The engineering properties of the foundation and embankment materials, obtained from laboratory testing, are summarized in Tables 1 and 2, respectively. Based on the Unified Soil Classification System (USCS), the kaolin clay is classified as low-plasticity clay (CL). The grain size distribution curve of kaolin clay and embankment soil is presented in Fig. 1.

Table 1. Properties of foundation soil.

Property	Symbol	Unit	Value
Specific gravity	G_S	-	2.60
Liquid limit	w_L	%	41.20
Plasticity index	I_p	%	19.20
Maximum particle diameter	D_{max}	mm	0.15
Soil classification	-	-	CL

Table 2. Properties of embankment soil.

Property	Symbol	Unit	Value
Specific gravity	G_S	-	2.65
Optimum moisture content	OMC	%	8.45
Maximum dry unit weight	*MDD*	kN/m^3	18.22
Angle of internal friction	φ	°	34
Soil classification	-	-	SM

2.2 GGBS-dolomite-based geopolymer as a deep mix column

Dolomite (D) and ground granulated blast furnace slag (GGBS) were used as binder materials in this study and were procured from Tata Steel Limited, Jamshedpur, Jharkhand, India. The engineering properties of GGBS and dolomite are summarized in Table 3. The grain size distribution of GGBS and dolomite is presented in Fig. 1. Analytical-grade sodium hydroxide (NaOH) pellets with 99% purity were procured from a local supplier. An 8 M NaOH solution was prepared by dissolving 320 g of NaOH pellets in 1 L of distilled water. The alkali activator used in the geopolymerization process was sodium hydroxide (NaOH) and sodium silicate (Na_2SiO_3) solution. To evaluate the combined effect of dolomite and GGBS and curing durations, a NaOH: Na_2SiO_3 mass ratio of 25:75 was adopted, along with

GGBS: dolomite ratios of 20:0, 18:2, 16:4, and 14:6, considering a total precursor content of 20%. Curing periods of 7, 14, and 28 days were examined. The water content of the kaolin clay was maintained at its liquid limit to simulate in-situ field conditions. Based on previous recommendations [6,25], a liquid-to-precursor (L/P) ratio of 1 was selected. In addition, specimens stabilized with 20% OPC at the liquid limit were prepared as control samples for comparison. The unconfined compressive strength (UCS) tests were performed on the cured samples for different curing intervals as per ASTM D2166 [26], with the tests performed at a constant displacement rate of 1.2 mm/min.

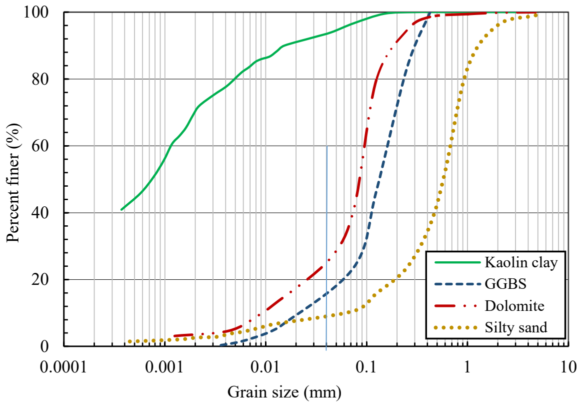

Fig. 1. Grain-size distribution curve for the kaolin clay, silty sand, GGBS, and dolomite.

Table 3. Engineering properties of GGBS and dolomite.

Property	Unit	GGBS	Dolomite
Specific gravity		2.80	2.82
D_{10}	mm	0.026	0.0087
D_{30}	mm	0.088	0.05
D_{60}	mm	0.17	0.10
c_u		6.54	2.00
c_c		1.75	2.87

2.3 Physical modelling

To investigate the response of untreated and geopolymer-treated soft clay supporting an embankment, a laboratory model study was conducted using a geometric scaling factor of 1:50 relative to the prototype. A rigid test tank with internal dimensions of 500 mm × 200 mm × 400 mm was fabricated for this purpose, as illustrated in Fig. 2a. The foundation bed consisted of soft clay prepared to an undrained shear strength of 5±1 kPa and placed to a depth of 240 mm. End-bearing geopolymer columns were installed within the clay bed with varying area replacement ratios (A_r). The optimum mix proportion of geopolymer-stabilized soft soil was obtained from the UCS test results, and that mix proportion was used for the preparation of columns for laboratory modelling. The loading plate was not rigidly connected to the loading rod, and therefore was free to rotate slightly during loading. This allows the plate to adjust to minor surface irregularities and ensures a more uniform and realistic distribution of applied load onto the embankment surface. Short-term static loading under undrained conditions was applied using a servo-controlled pneumatic loading system with a capacity of 20 kN. The tests were performed in strain-controlled mode at a constant vertical displacement rate of 1 mm/min. Settlement of the footing was recorded using a linear variable differential transformer (LVDT) connected to a data acquisition system. Each test was terminated when the vertical settlement reached 50 mm.

(a)

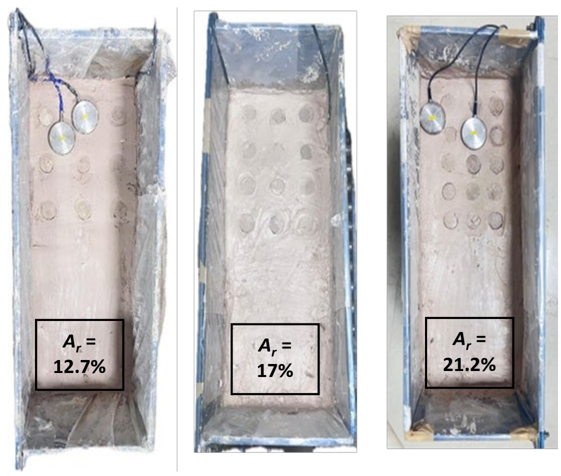

(b)

Fig. 2. (a) Model test setup, (b) Column installation for different A_r.

Owing to geometric symmetry, only half of the embankment–foundation system was modeled, following previous studies [27]. The embankment model had a height of 70 mm (equivalent to 3.5 m in the prototype), a crest width of 110 mm (5.5 m in the prototype), and side slopes of 1V:2H. In deep soil mixing (DSM) applications, column diameters typically range from 0.5 to 2.1 m, with center-to-center spacing of 1.0–1.5 m and lengths varying between 10 and 30 m [1,2]. Based on these ranges, a prototype geopolymer column diameter and length of 1.5 m and 12 m, respectively, were assumed, corresponding to a model column diameter of 30 mm and a height of 240 mm. The area replacement ratio (A_r), defined as the ratio of the total cross-sectional area of columns to the area of the treated ground, is a critical design parameter in DSM. Since A_r values in practice typically range between 10% and 30%, three representative values of 12.7%, 17%, and 21.2% were selected in this study. The columns were arranged in a square grid pattern, as shown in Fig. 2b.

2.4 Numerical modelling

The constitutive behavior of a GPSC-supported embankment resting on soft soil was analyzed using PLAXIS 3D. All components in the model test, namely the embankment, soft clay, and GPSCs (DSM columns), were modeled using quadratic 10-node tetrahedral elements. The model test tank of 0.5 m × 0.2 m × 0.4 m used in the experimental work was numerically modeled. The soil–column interaction was assumed as perfectly bonded (no slip condition). This assumption is justified as deep soil mixing produces in-situ mixed columns, leading to strong adhesion between soil and column material. Therefore, interface elements were not explicitly defined, and continuity was assumed between materials. The lateral boundaries allowed vertical displacement but restricted horizontal movement. The bottom boundary restricted movement in both the vertical and horizontal directions. Meanwhile, the model domain's top surface was free to move vertically in response to applied loads. Additionally, the embankment slope surface was not subject to any particular boundary conditions. The results from the finite element analysis were compared with those of the model tests. The initial vertical stress due to the gravity load was considered in the analysis.

The Mohr-Coulomb elastic-perfectly plastic model was used as the yield criterion for the geopolymer stabilized soil column, soft clay, and embankment soil. A linear elastic model is used to model the footing plate. For both soft soil and the GPSC, the undrained behavior is assumed, whereas the embankment soil is modeled to have drained behavior. The water content of the soil bed used in this investigation was 38% (liquid limit = 41.20%), at which the undrained shear strength was 5±1 kPa. Under undrained (c) conditions, the linear-elastic perfectly plastic Mohr-Coulomb criteria were used to simulate the behavior of soft soil. Table 4 presents the material parameters adopted for the numerical analysis.

A medium mesh density was used to discretize the embankment and associated model components. The modeled embankment construction and foundation system supported by GPSCs over soft soil are illustrated in Fig. 3.

Table 4. Engineering properties of materials used in finite element modelling.

Parameters	Soft soil	Geopolymer-stabilized soil column	Embankment soil
Constitutive model	MC	MC	MC
Specific Gravity, G_s	2.60	-	2.65
Unit weight, γ (kN/m^3)	16.08	18.50	18
Modulus of elasticity, E (kPa)	1110	88000	15000
Undrained shear strength, c_u (kPa)	5	264	3.80
Angle of internal friction, φ	-	31.50	34
Poison's ratio, ν	0.49	0.30	0.30

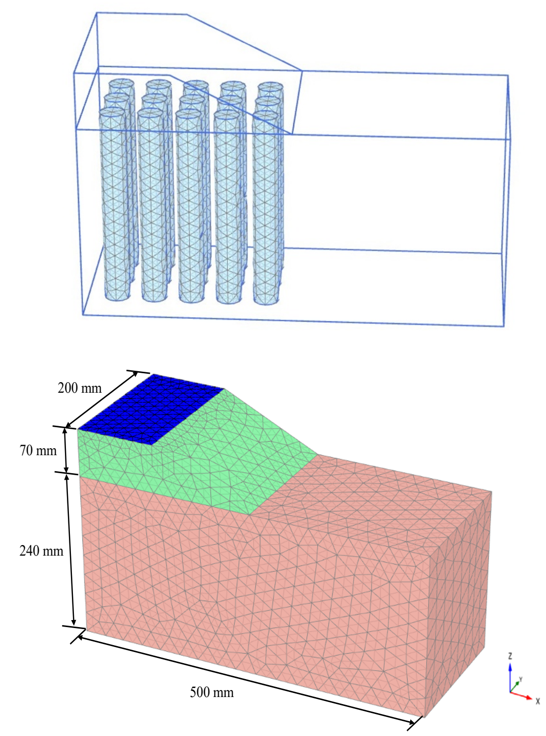

Fig. 3. Geometry of numerical model.

3 Results and discussion

3.1 Unconfined compressive strength

Fig. 4 presents the unconfined compressive strength (UCS) of cement and geopolymer-stabilized soft soil activated with an NH: NS mass ratio of 25:75, incorporating varying GGBS–dolomite proportions and cured for 7, 14, and 28 days. It was found that UCS increased with dolomite addition up to an optimum S:D ratio of 16:4, beyond which strength declined. The enhanced performance is attributed to increased alkalinity induced by dolomite, which promotes dissolution of amorphous silica and alumina from clay and GGBS, thereby increasing the availability of reactive Al^{3+} and Si^{4+} species necessary for geopolymeric gel formation [28]. Additionally, Ca^{2+} and Mg^{2+} released from dolomite accelerate geopolymerization kinetics by providing nucleation sites for hydration and gel precipitation, resulting in reduced setting time and enhanced matrix densification [10].

Replacement of GGBS with dolomite up to 4% significantly improved UCS, with the S16D4 mix exhibiting a 116.8% higher 28-day UCS compared to the GGBS-only geopolymer. Strength development showed strong curing dependency due to progressive geopolymeric gel formation and microstructural refinement. At 7 days, UCS of OPC20 specimens was comparable to S16D4 specimens; however, the latter exhibited higher strength gain rates, with UCS increases of 53.34% (7–14 days) and 93.80% (14–28 days), compared to 46.07% and 85.70%, respectively, for OPC20 specimens. These results indicate superior long-term strength development and reaction efficiency of the S16D4 geopolymer system relative to conventional OPC stabilization. OPC-treated specimens exhibited comparatively more brittle and sudden failure, with distinct shear planes. Geopolymer-treated specimens showed improved ductility at early curing stages, more uniform stress distribution, and gradual failure with enhanced energy absorption capacity. These differences are attributed to the formation of C-A-S-H and N-A-S-H gels in geopolymer systems, leading to improved microstructural integrity.

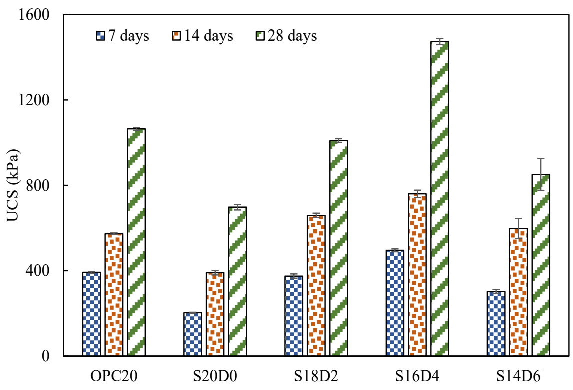

Fig. 4. Variation of unconfined compressive strength (UCS) of OPC and geopolymer-stabilized soft soil at different curing periods.

3.2 Response of embankment model tests

Fig. 5 illustrates the vertical stress–settlement behavior of the embankment model reinforced with end-bearing geopolymer-stabilized columns (GPSCs) and area replacement ratios (A_r) of 12.7%, 17%, and 21.2%. The performance was evaluated against an untreated soil embankment to quantify the effectiveness of ground improvement. The ultimate bearing capacity of the untreated soft soil bed was 25 kPa. The load-bearing capacity and stiffness of the embankment foundation system were significantly increased with the inclusion of GPSCs. The untreated soil primarily underwent localized shear failure along with surface heaving close to the loading region, whereas GPSCs inclusion showed general shear failure, indicating higher confinement and load distribution. As A_r increased, the ground's stiffness and ultimate bearing resistance increased, allowing it to withstand greater vertical stresses. The ultimate bearing capacity improved by 246.92%, 344.56%, and 418.80% for A_r values of 12.7%, 17%, and 21.2%, respectively, compared to untreated soil. The improved performance with increasing A_r is attributed to reduced column spacing and increased column cross-sectional area, which enhance load transfer efficiency and composite ground stiffness.

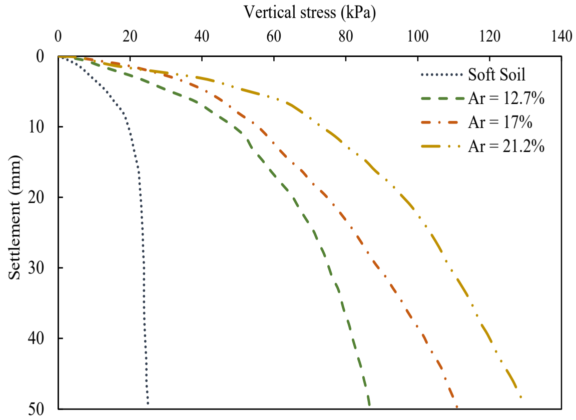

Fig. 5. Vertical stress-settlement curve for the unimproved and end-bearing GPSCs-improved embankment model.

3.3 Validation of laboratory model test results using FE model

The vertical stress-settlement behavior of a group of end-bearing GPSCs supported embankment for A_r of 12.7%, 17%, and 21.2% obtained from laboratory model studies and finite element modelling **is** shown in Fig. 6. A strong correlation was observed between the finite element simulation results and the experimental model test data for the embankment supported by a group of end-bearing GPSCs. The ultimate bearing capacity obtained from laboratory model tests for end-bearing GPSCs improved soft ground with A_r of 12.7%, 17%, and 21.2% is 86.73 kPa, 111.14 kPa, and 129.70 kPa, respectively, at 50 mm of settlement. The numerical validation marginally overpredicted the bearing capacity at lower settlement levels compared with the laboratory model test results. While the load intensity curve gradually increases with settlement up to 50 mm in the experimental studies, the Plaxis validations yield an ultimate load intensity of 85.84 kPa (at settlement of 46.56 mm), 108.96 kPa (at settlement of 46.08 mm), and 122.64 kPa (at settlement of 41.16 mm) for A_r of 12.7%, 17%, and 21.2% respectively.

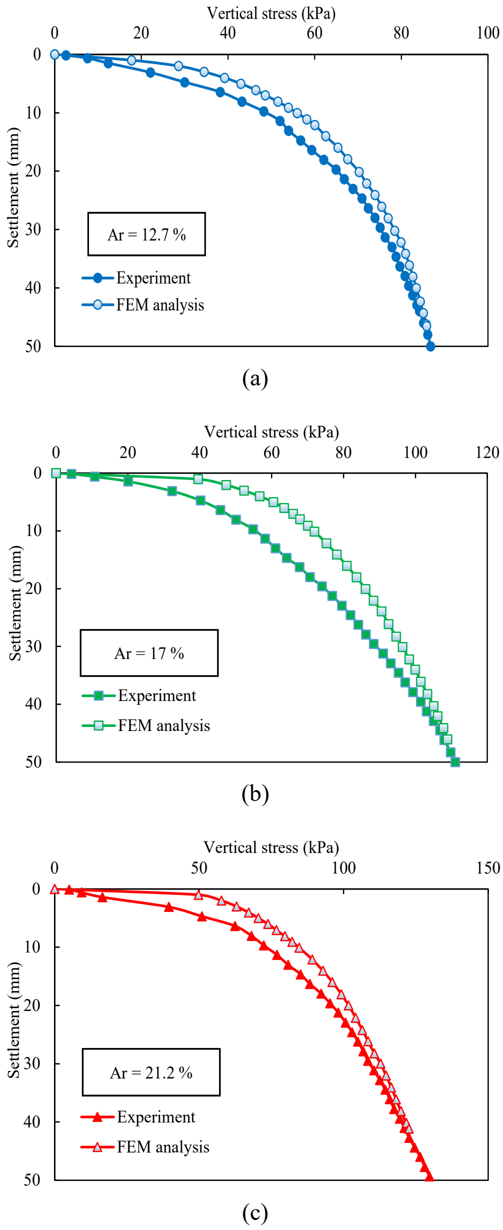

Fig. 6. Comparison of laboratory model test results and finite element predictions for embankment over end-bearing GPSCs-improved soft soil ground (Ar = 12.7% (a), 17% (b), and 21.2% (c)).

The displacement contours of different components of end-bearing GPSCs supported embankment on soft soil from finite element analysis at failure under static loading are shown in Fig. 7. The columns failed progressively during loading rather than undergoing simultaneous group failure, indicating interaction effects within the column group. The failure mechanism varied with the column location relative to the embankment geometry. GPSCs beneath the crest primarily experienced shear failure due to the concentration of vertical stresses, whereas columns beneath the embankment slope exhibited bending failure resulting from lateral soil movement and eccentric loading. At an A_r of 12.7%, due to larger spacing, the crest column exhibited shear failure, whereas the slope columns experienced limited outward displacement. As fewer columns participate in load sharing, it leads to lower stress concentration within the column group and reduced ultimate bearing capacity.

With an increase in A_r, the reduction in column spacing enhances group interaction and promotes the development of soil arching between adjacent columns. This improves load transfer efficiency and increases the stress concentration ratio within the GPSCs. As a result, columns beneath the slope region increasingly contribute to vertical load resistance and undergo outward bending due to lateral confinement effects. The combined increase in load sharing and composite ground stiffness leads to a significant improvement in the ultimate bearing capacity of the reinforced foundation system.

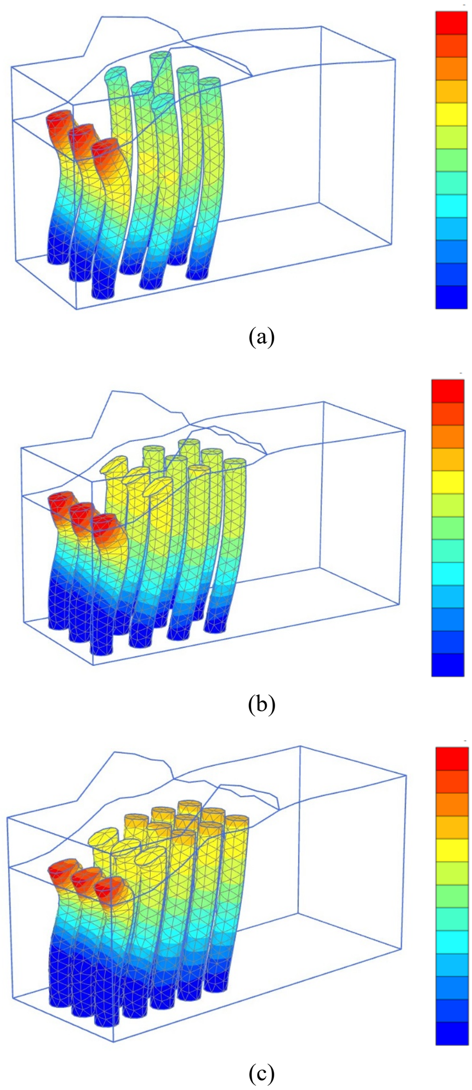

Fig. 7. Displacement contours of end-bearing GPSCs supported embankment model for A_r of (a) 12.7%, (b) 17%, and (c) 21.2%.

Fig. 8 shows the failure pattern of GPSC columns under embankment loading for an area replacement ratio of 21.2%. It can be seen that a similar failure pattern of GPSCs and total deformation mechanism was observed in the numerical analysis for the evaluated models, as compared to the laboratory model.

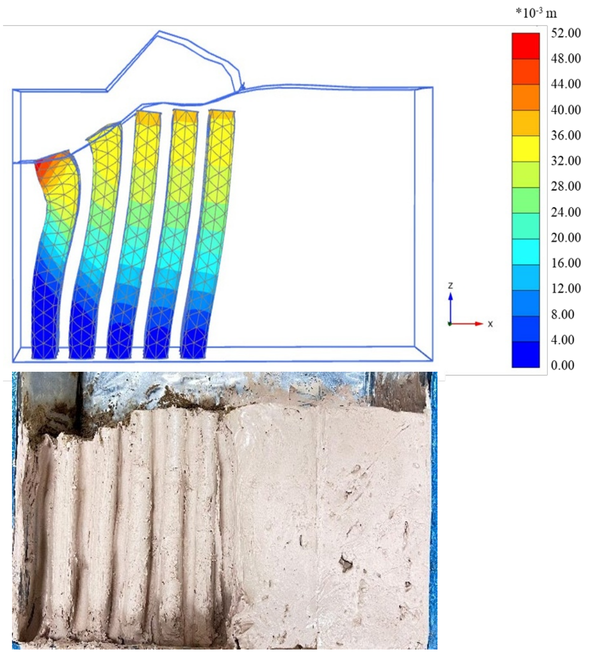

Fig. 8. Comparison of failure pattern of GPSCs with an area replacement ratio of 21.2% obtained from the FE model and laboratory model.

4 Conclusion

- The optimum GGBS: dolomite ratio of 16:4 yielded the highest UCS, showing 116.80% higher 28-day strength compared to GGBS-only geopolymer and demonstrating superior long-term strength gain compared to OPC stabilization.
- The ultimate bearing capacity of the embankment increased by 246.92%, 344.56%, and 418.80% for area replacement ratios of 12.7%, 17%, and 21.2%, respectively, due to improved load transfer and composite ground stiffness.
- Increasing the area replacement ratio reduces column spacing, enhances stress redistribution, and improves load sharing, resulting in higher stiffness and bearing capacity of the reinforced ground.
- FE model predictions closely captured the stress–settlement response and failure mechanisms, confirming the reliability of numerical modeling for analyzing GPSC-supported embankments.

References

1. M. Kitazume, M. Terashi, The Deep Mixing Method, CRC Press, London (2013).
2. S. Gupta, S. Kumar, A state-of-the-art review of the deep soil mixing technique for ground improvement, Innovative Infrastructure Solutions **8**, 129 (2023). https://doi.org/10.1007/s41062-023-01098-6.
3. J. Davidovits, Geopolymers - Inorganic polymeric new materials, Journal of Thermal Analysis **37**, 1633–1656 (1991). https://doi.org/10.1007/BF01912193.
4. S. Gupta, S. Kumar, Dynamic behavior of geopolymer stabilized kaolin clay under long-term cyclic loading, Constr. Build. Mater. **407**, 133562 (2023). https://doi.org/10.1016/j.conbuildmat.2023.133562.
5. S. Gupta, S. Kumar, Mechanical and microstructural analysis of soft kaolin clay stabilized by GGBS and dolomite-based geopolymer, Constr. Build. Mater. **421**, 135702 (2024). https://doi.org/10.1016/j.conbuildmat.2024.135702.
6. M. Yaghoubi, A. Arulrajah, S. Horpibulsuk, Engineering Behaviour of a Geopolymer-stabilised High-water Content Soft Clay, International Journal of Geosynthetics and Ground Engineering **8**, 45 (2022). https://doi.org/10.1007/s40891-022-00385-z.
7. H. Zhou, X. Wang, Y. Wu, X. Zhang, Mechanical properties and micro-mechanisms of marine soft soil stabilized by different calcium content precursors based geopolymers, Constr. Build. Mater. **305**, 124722 (2021). https://doi.org/10.1016/j.conbuildmat.2021.124722.
8. J. Davidovits, Application of Ca-based geopolymer with blast furnace slag, a review, in proceedings of 2nd International Slag Valorisation Symposium, 33-49 (2011).
9. A. Machner, M. Zajac, M. Ben Haha, K.O. Kjellsen, M.R. Geiker, K. De Weerdt, Stability of the hydrate phase assemblage in Portland composite cements containing dolomite and metakaolin after leaching, carbonation, and chloride exposure, Cem. Concr. Compos. **89**, 89–106 (2018). https://doi.org/10.1016/j.cemconcomp.2018.02.013.
10. H. Ye, C. Fu, G. Yang, Influence of dolomite on the properties and microstructure of alkali-activated slag with and without pulverized fly ash, Cem. Concr. Compos. **103**, 224–232 (2019). https://doi.org/10.1016/j.cemconcomp.2019.05.011.
11. H. Ye, C. Fu, G. Yang, Alkali-activated slag substituted by metakaolin and dolomite at 20 and 50°C, Cem. Concr. Compos. **105**, 103442 (2020). https://doi.org/10.1016/j.cemconcomp.2019.103442.
12. J. Chai, S. Shrestha, T. Hino, Failure of an Embankment on Soil-Cement Column–Improved Clay Deposit: Investigation and Analysis, Journal of Geotechnical and Geoenvironmental Engineering **145** (2019). https://doi.org/10.1061/(asce)gt.1943-5606.0002118.
13. J. Chai, S. Pongsivasathit, A method for predicting consolidation settlements of floating column improved clayey subsoil, Frontiers of Architecture and Civil Engineering in China **4**, 241–251 (2010). https://doi.org/10.1007/s11709-010-0024-3.
14. A. Dehghanbanadaki, A.S.A. Rashid, K. Ahmad, N.Z.M. Yunus, J.T. Shahu, M. Mohanty, Ultimate Bearing Capacity of Soft Soil Improved by DCM Columns: A Comparative Review, KSCE Journal of Civil Engineering **26**, 2653–2661 (2022). https://doi.org/10.1007/s12205-022-1463-9.
15. A.R. Bunawan, E. Momeni, D.J. Armaghani, K. Nissa binti Mat Said, A.S.A. Rashid, Experimental and intelligent techniques to estimate bearing capacity of cohesive soft soils reinforced with soil-cement columns, Measurement (Lond). **124**, 529–538 (2018). https://doi.org/10.1016/j.measurement.2018.04.057.
16. J.-H. Yin, Z. Fang, Physical modelling of consolidation behaviour of a composite foundation consisting of a cement-mixed soil column and untreated soft marine clay, Géotechnique **56** (1): 63–68 (2006). https://doi.org/10.1680/geot.2006.56.1.63
17. J.C. Chai, S. Shrestha, T. Hino, W.Q. Ding, Y. Kamo, J. Carter, 2D and 3D analyses of an embankment on clay improved by soil–cement columns, Comput. Geotech. **68**, 28–37 (2015). https://doi.org/10.1016/J.COMPGEO.2015.03.014.
18. P. Jamsawang, N. Yoobanpot, N. Thanasisathit, P. Voottipruex, P. Jongpradist, Three-dimensional

numerical analysis of a DCM column-supported highway embankment, Comput. Geotech. **72**, 42–56 (2016). https://doi.org/10.1016/j.compgeo.2015.11.006.

19. P. Ni, Y. Yi, S. Liu, Bearing capacity of composite ground with soil-cement columns under earth fills: Physical and numerical modeling, Soils and Foundations **59**, 2206–2219 (2019). https://doi.org/10.1016/j.sandf.2019.12.004.
20. N.N.S. Yapage, D.S. Liyanapathirana, H.G. Poulos, R.B. Kelly, C.J. Leo, Numerical Modeling of Geotextile-Reinforced Embankments over Deep Cement Mixed Columns Incorporating Strain-Softening Behavior of Columns, International Journal of Geomechanics **15** (2015). https://doi.org/10.1061/(asce)gm.1943-5622.0000341.
21. S. Horpibulsuk, A. Chinkulkijniwat, A. Cholphatsorn, J. Suebsuk, M.D. Liu, Consolidation behavior of soil-cement column improved ground, Comput. Geotech. **43**, 37–50 (2012). https://doi.org/10.1016/j.compgeo.2012.02.003.
22. Y. Jiang, J. Han, G. Zheng, Numerical analysis of consolidation of soft soils fully-penetrated by deep-mixed columns, KSCE Journal of Civil Engineering **17**, 96–105 (2013). https://doi.org/10.1007/s12205-013-1641-x.
23. S. Liu, D. Zhang, T. Song, G. Zhang, L. Fan, A Method of Settlement Calculation of Ground Improved by Floating Deep Mixed Columns Based on Laboratory Model Tests and Finite Element Analysis, International Journal of Civil Engineering **20**, 207–222 (2022). https://doi.org/10.1007/s40999-021-00662-4.
24. S. Horpibulsuk, R. Rachan, A. Suddeepong, State of the art in strength development of soil-cement columns, Proceedings of the Institution of Civil Engineers: Ground Improvement **165**, 201–215 (2012). https://doi.org/10.1680/grim.11.00006.
25. S. Horpibulsuk, N. Miura, T.S. Nagaraj, Clay–Water⁄Cement Ratio Identity for Cement Admixed Soft Clays, Journal of Geotechnical and Geoenvironmental Engineering **131**, 187–192 (2005). https://doi.org/10.1061/(asce)1090-0241(2005)131:2(187).
26. ASTM D2166M - 16, Standard Specification for Unconfined Compressive Strength of Cohesive Soil (D2166/D2166M − 16). American Society for Testing and Materials (ASTM) International, West Conshohocken, PA. (2016). https://doi.org/10.1520/D2166.
27. M.Y. Fattah, M.A. Al-Neami, A. Shamel Al-Suhaily, Estimation of bearing capacity of floating group of stone columns, Engineering Science and Technology, an International Journal **20**, 1166–1172 (2017). https://doi.org/10.1016/j.jestch.2017.03.005.
28. A. Arulrajah, M. Yaghoubi, M.M. Disfani, S. Horpibulsuk, M.W. Bo, M. Leong, Evaluation of fly ash- and slag-based geopolymers for the improvement of a soft marine clay by deep soil mixing, Soils and Foundations **58**, 1358–1370 (2018). https://doi.org/10.1016/j.sandf.2018.07.005.